International Journal of Earth, Energy and Environmental Sciences
ISSN: 2517-942X
Vol:7, No:12, 2013

Selection of Appropriate Classification Technique for Lithological Mapping of Gali Jagir Area, Pakistan

Khunsa Fatima, Umar K. Khattak, Allah Bakhsh Kausar

***Abstract*—**Satellite images interpretation and analysis assist geologists by providing valuable information about geology and minerals of an area to be surveyed. A test site in Fatejang of district Attock has been studied using Landsat ETM+ and ASTER satellite images for lithological mapping. Five different supervised image classification techniques namely maximum likelihood, parallelepiped, minimum distance to mean, mahalanobis distance and spectral angle mapper have been performed upon both satellite data images to find out the suitable classification technique for lithological mapping in the study area. Results of these five image classification techniques were compared with the geological map produced by Geological Survey of Pakistan. Result of maximum likelihood classification technique applied on ASTER satellite image has highest correlation of 0.66 with the geological map. Field observations and XRD spectra of field samples also verified the results. A lithological map was then prepared based on the maximum likelihood classification of ASTER satellite image.

***Keywords*—**ASTER, Landsat-ETM+, Satellite, Image classification.

I. Introduction

IN the last few decades, satellite data have been used extensively for lithological mapping and mineral exploration [1]-[5]. Landsat data have been used for a number of geological applications like faults and lineaments mapping, surface lithological discrimination, mineral exploration and exploitation [1], [2], [6]-[8]. After the launch of ASTER satellite in December 2009, due to its better spatial (15m) and spectral (14 bands) resolution, ASTER data are widely used for lithological and mineral mapping [9]-[12].

The current research study demonstrates the potential and applicability of remote sensing techniques and data for lithological mapping using two different optical sensors: Landsat-ETM+ and ASTER, that are different in their spatial and spectral resolution. Another aspect of this research study is to develop a geological map based on most suitable image classification technique. A number of image classification techniques have been utilized for lithological mapping. Maximum likelihood classification (MLC) has applied on Landsat-ETM+ satellite image to distinguish altered zoned classes from the unaltered fresh rocks [6] and to discriminate lithological units in vegetated Granite-Gneiss terrain [13].

Khunsa Fatima is with National University of Sciences and Technology, Islamabad, Pakistan (phone: +92-051-90854492, e-mail: khunsafatima@gmail.com).

Umar K Khattak, Dr., is with National University of Sciences and Technology, Islamabad, Pakistan (e-mail: ukhattak@hotmail.com).

Allah Bakhsh Kausar, Dr, was with Geological Survey of Pakistan. He is now with COMSATS Abbottabad, Pakistan (e-mail: Kausar_20001@yahoo.com).

Funds and laboratory equipment to conduct this research work was provided by National University of Sciences and Technology, Islamabad, Pakistan.

II. Study Area

Proposed study area for the current research work is GaliJagir area, tehsil Fatehjang, district Attock. The accessibility to this area is from Rawalpindi via Tarnol to Fatehjang (17km from study area). Main focus in this research study is upon Khaira Murat Range (KMR) that contains Marine deposits of Eocene age; divided into Margalla Hill Formation (PMh), ChorGali Formation (PCh) and Kuldana Formation (PKu). Major rock types are limestone, claystone, sandstone, siltstone and shale. Dominant minerals of the study area are calcite, quartz and montmorillonite/bentonite [14].

TABLE I
Stratigraphic Sequence of the Study Area [2]

Era	Period	Epoch	Age (mya)	Formation	Lithology
CAINOZOIC	Quaternary	Holocene	Present to 0.01	Potowar Clay	Clay
				Alluvium	Sand, Silt, Clay
		Pleistocene	1.8	Unconformity	
	Tertiary	Pliocene	5	Chinji	Mudstone, Sandstone
		Miocene	24	Kamlial	Sandstone, Clay
				Murree	Sandstone, Siltstone, Conglomerate
		Oligocene	73	Unconformity	
		Eocene	54	Chorgali	Shale, Limestone, Marl
				Margalla Hill Limestone	Limestone
		Paleocene	65		

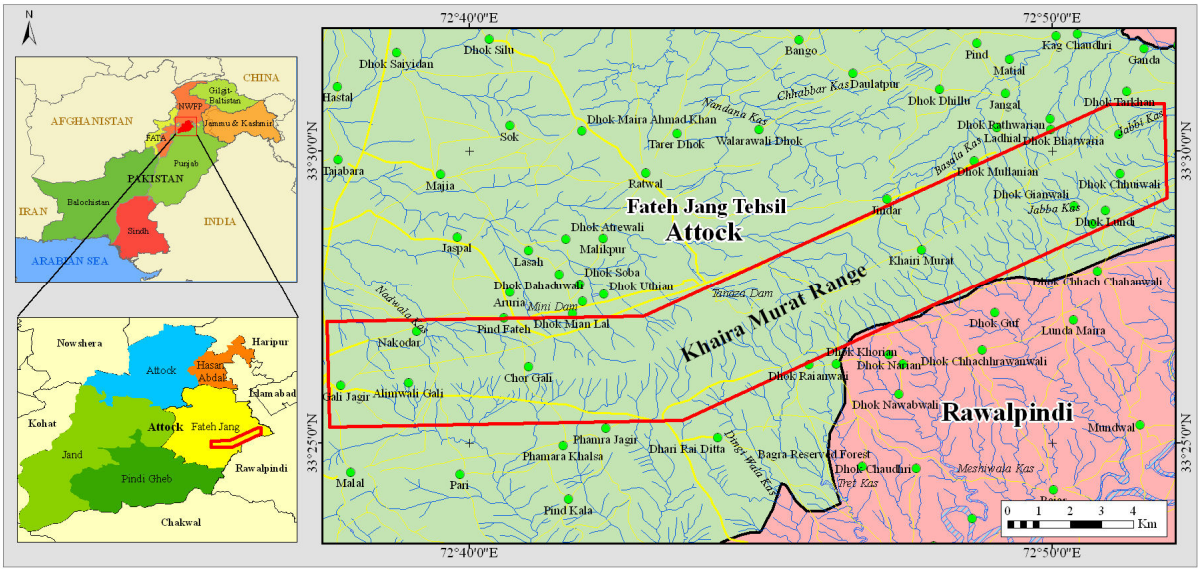

Fig. 1 Geographical map of Khaira Murat Mountain Range area, tehsil Fatehjang, district Attock , showing roads, water channels and villages. It is digitized from survey of Pakistan topographic sheets (43C-10, 43C-11, 43C-14 and 43C-15) at a scale of 1:50,000. Streams emanating from the uplands of Khaira Murat Range can be noticed. On the northern slopes, the streams flow roughly northwards, whereas on the southern slopes they flow southward and southeastward. The study area is outlined as red

III. Materials and Methods

Materials used in this research study include primary data in the form of satellite images of Landsat –ETM+ and ASTER data, and ancillary data like topographic maps (at 1:50'000 scale) of Survey of Pakistan and geological map (at 1:50'000 scale) of Geological Survey of Pakistan. Landsat-ETM+ data have total 8 spectral bands with spatial resolution of 30m (3 visible bands, 1 NIR band, 2 SWIR bands), 60m (1TIR band), and 15m (1panchromatic band).Visible, NIR, SWRI and TIR bands of Landsat-ETM+ were pan sharpened to have 15m spatial resolution. ASTER data have 14 spectral bands (4 VNIR bands, 6 SWIR bands, and 5 TIR bands). SWIR and TIR bands of ASTER data were also pan sharpened to have 15m resolution.

Both primary and ancillary data are geo-referenced and have assigned World Geodetic System (WGS) 1984. As ASTER thermal bands have high band correlation, de-correlation stretch algorithm has been proposed to reduce the TIR bands correlation [15]. For ASTER, de-correlation stretched images are used in supervised image classification techniques. Accuracy of lithological mapping by five supervised classification is then assessed by field survey and by comparing them with Geological Survey of Pakistan map. The most appropriate image classification technique leads to the generation of geological map. Printed SOP sheets, classified maps, GPS and binoculars were used in the field survey.

IV. GIS Analysis

The current research study focuses on the application of image classification techniques in analyzing remotely sensed data for lithological characterization mapping. Five supervised image classification techniques namely MLC, MDMC, MHDC, PPC and SAM are applied on the Landsat-ETM+ and ASTER data images. The accuracy of these classification techniques was accessed by determining their correlation coefficient R^2 with the geological map produced by Geological Survey of Pakistan. The most suitable classification technique was then verified by field observations and XRD spectra of field samples.

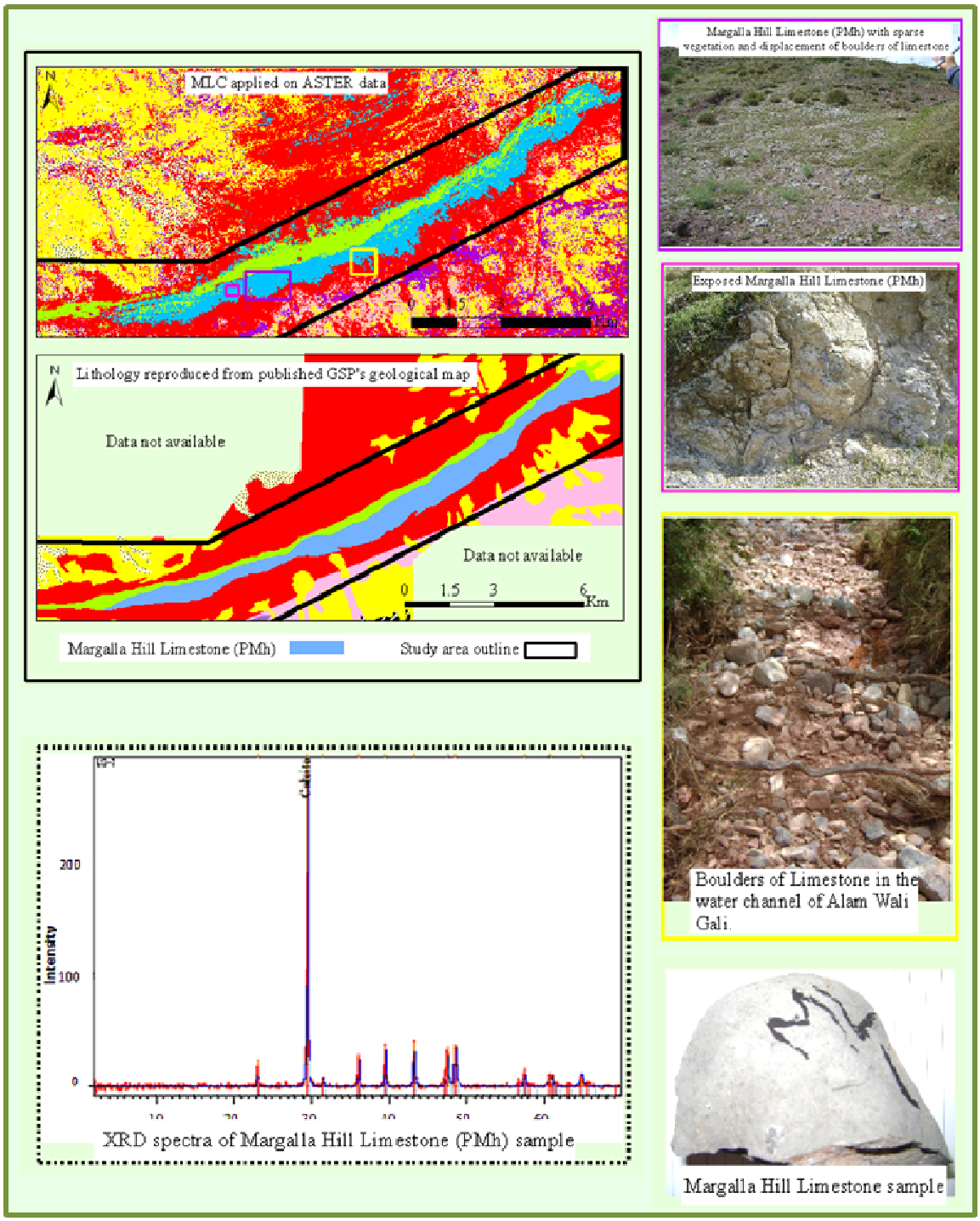

Fig. 2 Validation of Margalla Hill Formation (PMh) mapped by maximum likelihood classification (MLC) applied on ASTER data satellite image by comparing with GSP's geological map, field survey and XRD spectra of the collected samples. Magenta frame shows the exposed limestone in the study area. Yellow frame highlights that in ASTER data MLC picked Margalla Hill Limestone in nallahs due to the displaced limestone boulders in them

Supervised image classification is the procedure that is used for the analysis of remote sensing multispectral image data. It uses suitable algorithms to label specific pixels in an image as representative ground cover classes. Band combination of RGB (742) was used to apply five supervised image classification techniques on both Landsat-ETM+ and ASTER data satellite

images. Training areas were defined based upon knowledge of the published geological map of GSP. Results of supervised image classification were then compared with GSP's geological map by determining correlation coefficients R^2. 200 random points were selected in the study area of Khaira Murat range. Lithology mapped by different supervised image classification techniques was recorded at these random points. Correlation coefficients R^2 of these random points were then determined between GSP and different supervised image classification techniques mapped by ASTER and Landsat-ETM+ (Table II). The correlation coefficients for the comparative analysis show that the MLC of ASTER data has the highest correlation with the GSP data as compared to the rest of the classification techniques. Due to better spectral resolution (14 spectral bands) of ASTER, supervised image classification techniques applied on ASTER showed higher correlation with GSP as compared to Landsat-ETM+ based classification techniques. Also, the increased numbers of SWIR and TIR bands of ASTER satellite data enhanced the capability for lithological discrimination as compared to Landsat-TM data. A geological map is then constructed based upon the MLC of ASTER satellite data (Fig. 6).

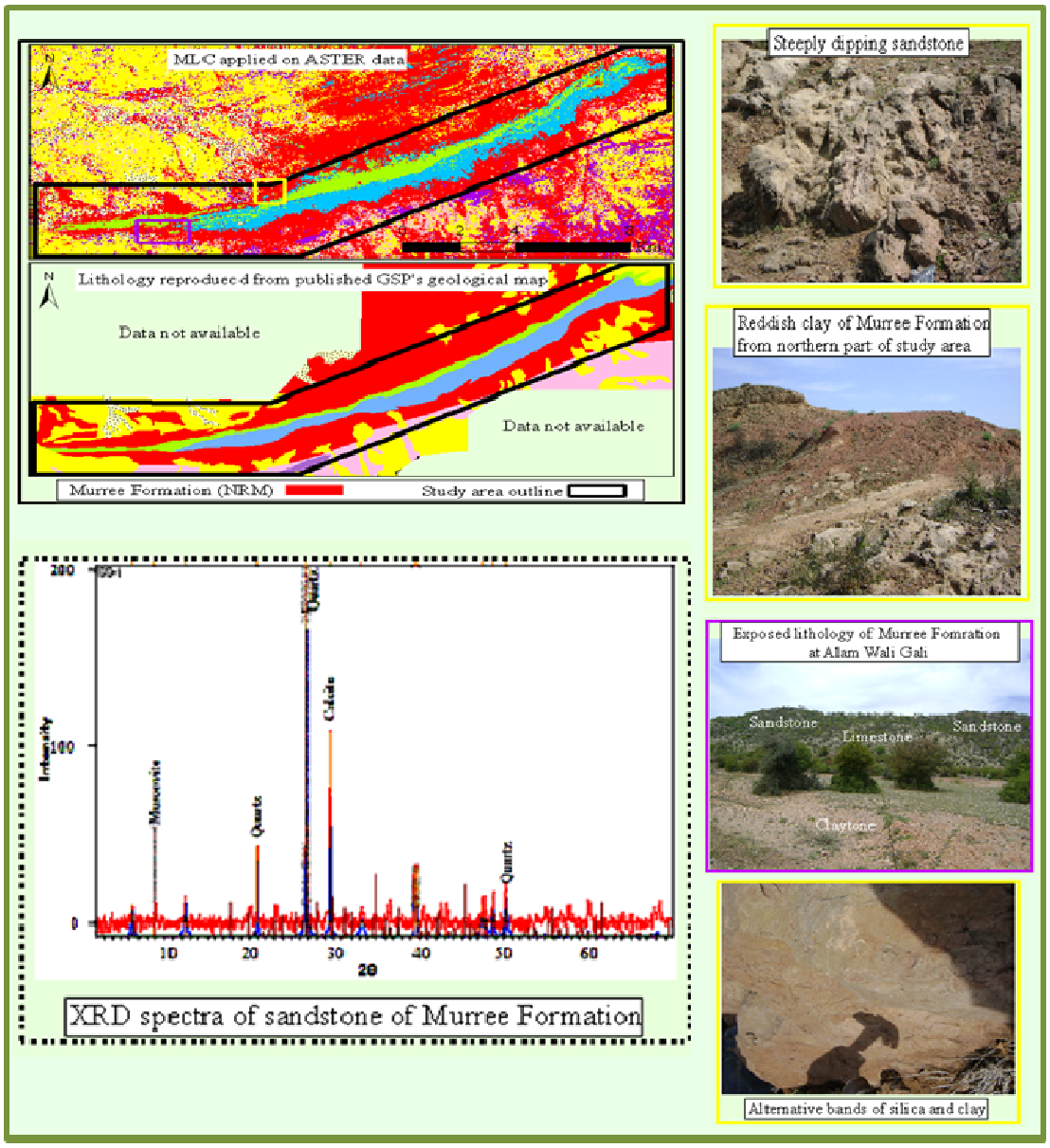

Fig. 3 Validation of Murree Formation mapped by maximum likelihood classification (MLC) on ASTER data satellite image by comparing with GSP's geological map, field survey and XRD spectra of the sandstone samples. Yellow frames show sandstone and clay outcrops in the study area classified as Murree Formation. Alternative bands of silica and clay are also present in the study area

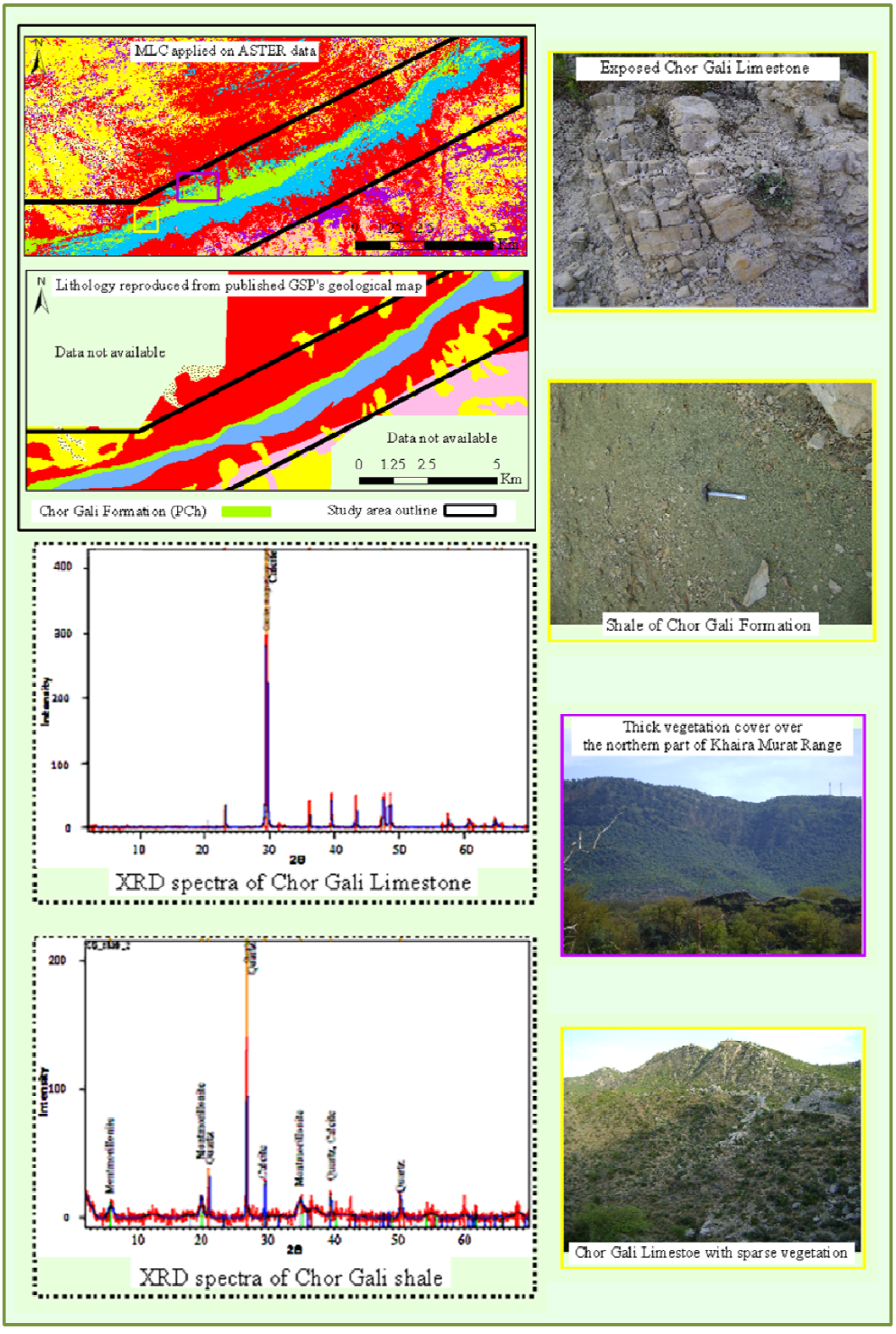

Fig. 4 Validation of ChorGali Formation mapped by maximum likelihood classification (MLC) on ASTER data satellite image by comparing with GSP's geological map, field survey and XRD spectra of the limestone and shale samples collected during field survey. Yellow frame shows exposed limestone and shale in ChorGali Formation. Some mismatch in area estimation is probably due to partial vegetation cover over a lithology or due to displacement of boulders and pebbles of a different rock type over a formation

TABLE II
CORRELATION COEFFICIENTS AMONG LITHOLOGIES MAPPED BY GSP AND BY DIFFERENT SUPERVISED IMAGE CLASSIFICATION TECHNIQUES USING ON LANDSAT-ETM+ AND ASTER SATELLITE IMAGES

Correlation Coefficient		GSP
GSP		1.00
ASTER	MLC	0.66
	MDMC	0.55
	MHDC	0.58
	PPC	0.56
	SAM	0.58
Landsat-ETM+	MLC	0.43
	MDMC	0.47
	MHDC	0.39
	PPC	0.43
	SAM	0.31

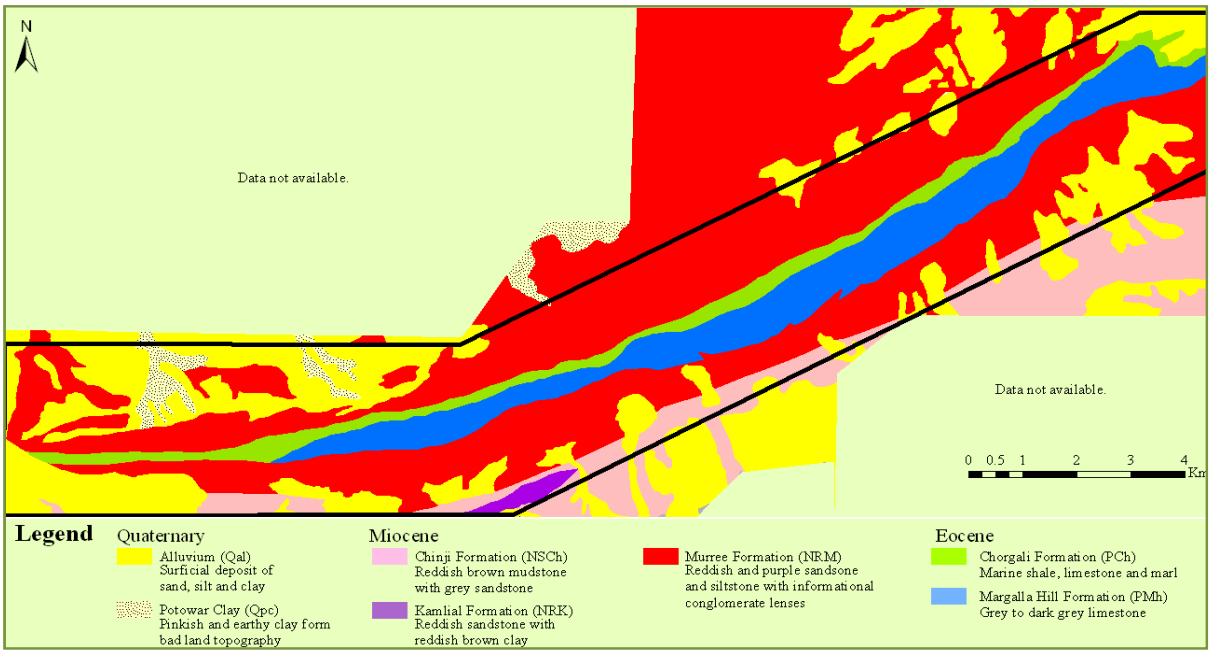

Fig. 5 Lithological nap reproduced from Geological Survey of Pakistan's "Geological Map of Khaira Murat Range, district Attock" at a scale of 1: 50,000 [14]. Geological age of the formations in the mapped area is Cainozoic, which is subdivided into Quaternary, Neogene and Paleogene periods. The study area contains five lithological formations. Margalla Hill Formation and ChorGali Formation are oldest and lie in the Paleogene Period. Chinji Formation, Kamlial Formation and Murree Formation lie in the Neogene Period. Alluvium and Potwar Clay lie in the recent Quaternary period. Study area is outlined

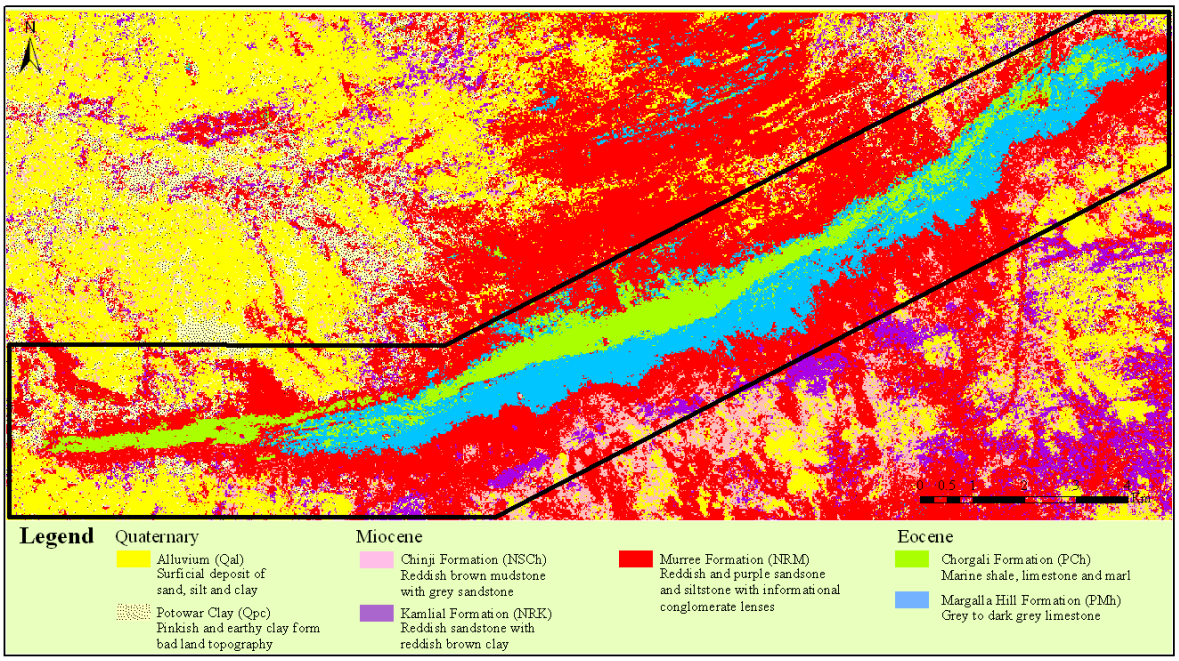

Fig. 6 Lithological map produced from maximum likelihood classification of ASTER data. Study area is outlined. Khaira Murat range is classified as Margalla Hill Formation and ChorGali Formation which lie in the Paleogene of the Cainozoic Era. Margalla Hill Limestone can be seen in the southern nallahs. Murree Formation of Neogene Period is classified on both sides of the Khaira Murat range. Both Kamlial Formation and Chinji Formation are classified in the southern part. The recent lithologies of Quaternary Period i.e. Alluvium and Potwar Clay commonly occur in the north western side; however it can be seen in patches throughout the area

V. Results and Discussions

The discrepancies between the satellites based lithological map (Fig. 6) and lithological map reproduced from GSP's geological map (Fig. 5) is due to difference in the method of their preparation. GSP's geological maps are produced at a scale of 1:50,000 by extensive field surveys and provide a generally smoother look of different lithologies. While the satellite based lithological maps are based upon the spectral reflectance of different lithologies due to which it reveals the complex distribution of different lithologies. Also the lithological map in the current research study is produced from ASTER data at a spatial resolution of 15m. Vegetation cover and displaced boulders in the drainage beds cover the underlying lithology.

Field observations in the study area support the results obtained from remote sensing techniques for lithological mapping; when Landsat-ETM+ and ASTER data images were used in combination with secondary data like published geological maps. Lithological map of the study area created from supervised image classification technique and band ratioing demonstrated the benefits of Landsat-ETM+ and ASTER data images.

Supervised image classification techniques applied on ASTER data image demonstrated that MLC was the most suitable classification technique for lithological mapping of the study area. ASTER data, due to its finer spectral resolution than Landsat-ETM+, provided better results for lithological mapping than Landsat-ETM+.

Since spectral bands of ASTER data have very high correlation between them, different image enhancement algorithms were applied on ASTER data satellite image which proved significant for geological study. De-correlation stretched algorithm greatly enhanced the geological features of the study area and made the ASTER data image more visually interpretable for supervised image classification. Log residual algorithm increased the spectral range of the image and thus the slight spectral characteristics of certain minerals were greatly enhanced. This led to the successful application of band ratio indices for mineral exploration.

VI. Recommendations

Satellite based data like Landsat-ETM+ and ASTER data have limitation of alluvial and vegetation cover. This limitation may be overcome by using Radar data in combination with satellite based data; as Radar waves may penetrate through thick vegetation and even the soil [16].

Remote sensing techniques explored may be applied in remote and inaccessible areas to help delineate geological formations at the surface. A sketch about the geology of an area under investigation may be drawn to limit the area for surveying and to target specific minerals. Maximum likelihood classification proved to be most suitable in this study area. Other areas may be discernable with some other classification technique.

ASTER data has fewer SWIR bands as compared to EO-1 Hyperion data (144 spectral bands). Thus Hyperion may better

discriminate among different mineral types. However, the latter has a low signal-to-noise ratio [17]. A case study utilizing both ASTER and EO-1 Hyperion data may be useful for comparing the capabilities of the two sensors' data.

REFERENCES

[1] H. A. El-Etr and M. S. M. Yousif, "Utilization of "Landsat" images and conventional aerial photographs in the delineation of some aspects of the geology of the central eastern desert, Egypt," *Precambrian Research,* vol. 6, pp. A14-A15, 1978.

[2] I. Kayan and V. Klemas, "Application of LANDSAT imagery to studies of structural geology and geomorphology of the Mentese region of southwestern Turkey," *Remote Sensing of Environment,* vol. 7, pp. 51-60, 1978.

[3] M. Hashim, S. Ahmad, M. A. M. Johari, and A. B. Pour, "Automatic lineament extraction in a heavily vegetated region using Landsat Enhanced Thematic Mapper (ETM+) imagery," *Advances in Space Research,* vol. 51, pp. 874-890, 2013.

[4] P. A. Davis, C. S. Breed, J. F. McCauley, and G. G. Schaber, "Surficial geology of the Safsaf region, south-central Egypt, derived from remote-sensing and field data," *Remote Sensing of Environment,* vol. 46, pp. 183-203, 1993.

[5] F. F. Sabins, "Remote sensing for mineral exploration," *Ore Geology Reviews,* vol. 14, pp. 157-183, 1999.

[6] I. A. A. B. Sami O. El Khidir, "Digital Image Processing and Geospatial Analysis of Landsat 7 ETM+ for Mineral Exploration, Abidiya area, Northern Sudan," *International Journal of Geomatics and Geosciences,* vol. 3, p. 14, March 2013 2013.

[7] A. N. R. J.R.Harris, B.Ballantyne, C. Sheridon, "Mapping Altered Rocks using Landsat TM and Lithogeochemical Data: Sulphurets-Brucejack Lake District, British Columbia, Canada," *Photogrammetric Engineering and Remote Sensing,* vol. 64, p. 14, April 19988 1998.

[8] Y. F. MD.Bodruddoza Mia, "Mapping Hydrothermal Altered Mineral Deposits using Landsat 7 ETM+ Image in and around Kuju Volcano, Kyushu, Japan," *Journal of Earth System Science,* vol. 121, p. 9, August 2012 2012.

[9] F. Qiu, M. Abdelsalam, and P. Thakkar, "Spectral analysis of ASTER data covering part of the Neoproterozoic Allaqi-Heiani suture, Southern Egypt," *Journal of African Earth Sciences,* vol. 44, pp. 169-180, 2006.

[10] C. D. Cecile Gomez, Pascal Allemand, Patrick Ledru, R. Wackerle, "Using ASTER Remote Sensing Data Set for Geological Mapping in Namibia," *Physics and Chemistry of the Earth,* p. 12, 24 August 2004 2004.

[11] A. B. Pour and M. Hashim, "The application of ASTER remote sensing data to porphyry copper and epithermal gold deposits," *Ore Geology Reviews,* vol. 44, pp. 1-9, 2012.

[12] A. L. H. Asadi Haroni, "Integrated Analysis of ASTER and Landsat ETM Data to Map Exploration Targets in the Muteh Gold-Mining area, Iran," *ISPRS Journal of Photogrammetry and Remote Sensing,* vol. XXXVI, p. 4, June 2007 2007.

[13] E. M. Schetselaar, C.-J. F. Chung, and K. E. Kim, "Integration of Landsat TM, Gamma-Ray, Magnetic, and Field Data to Discriminate Lithological Units in Vegetated," *Remote Sensing of Environment,* vol. 71, pp. 89-105, 2000.

[14] M. Latif, Hussain, H, " Limestone quarry sites around Islamabad and Kohat," *Geological Survey of Pakistan,* vol. 721-722, 2002.

[15] A. Gillespie, "Enhancement of multispectral thermal infrared images: Decorrelation contrast stretching " *Remote Sensing of Environment,* vol. 42, p. 9, 1992.

[16] T. Raharimahefa and T. M. Kusky, "Structural and remote sensing analysis of the Betsimisaraka Suture in northeastern Madagascar," *Gondwana Research,* vol. 15, pp. 14-27, 2009.

[17] A. Moghtaderi, Moore, F., & Mohammadzadeh, A. , "The application of advanced space-borne thermal emission and reflection (ASTER) radiometer data in the detection of alteration in the Chadormalu paleocrater, Bafq region, Central Iran," *Journal of Asian Earth Sciences,* vol. 30, p. 15, 2007.